Remote Sensing of Environment 245 (2020) 111795

Contents lists available at ScienceDirect

Remote Sensing of Environment

journal homepage: www.elsevier.com/locate/rse

Water-related ecosystems' mapping and assessment based on remote sensing techniques and geospatial analysis: The SWOS national service case of the Greek Ramsar sites and their catchments

Eleni Fitoka[a,*], Maria Tompoulidou[a], Lena Hatziiordanou[a], Antonis Apostolakis[a], Rene Höfer[b], Kathrin Weise[b], Charalampos Ververis[c]

[a] The Goulandris Natural History Museum - Greek Biotope Wetland Centre (EKBY), Greece
[b] Jena Optronik GmbH, Germany
[c] Ministry of Environment and Energy, Department of Protected Areas, Greece

ARTICLE INFO

Edited by Emilio Chuvieco

Keywords:
Wetland ecosystem extent
Object based image analysis
Sentinel 2MSI
Landsat 5TM
SDG 6.6.1 indicator
Ramsar convention
MAES nomenclature

ABSTRACT

Mapping and assessment of water-related ecosystems is a challenging task that requires advanced processing techniques with clear rules and standards in terminology and definition of class features. These ecosystems are hydrologically and ecologically connected at catchment level and co-exist within a human context. The SWOS (Satellite based Wetland Observation Service - Horizon 2020) national service case for mapping and assessing the 10 Greek Ramsar wetland sites and their catchment areas is built on the requirements of the Ramsar Convention on Wetlands and of the Aichi Biodiversity Targets of the Strategic Plan for Biodiversity 2011–2020. It contributes directly to Sustainable Development Goal (SDG) Global Indicator 6.6.1 "Sub-Indicator 1 – spatial extent of water-related ecosystems". An Object-Based Image Analysis (OBIA) approach was adopted using Sentinel-2 satellite images for the year 2017, to discriminate 31 classes (wetland and non-wetland) over an area of 2,015,591 ha. The classification model was further adjusted to Landsat 5 TM imagery of previous years (1986–1987) in order to extract possible changes in the spatial extent of water-related ecosystems. The Mapping and Assessment of Ecosystems and their Services (MAES) ecosystem typology, as this was enhanced within SWOS, was applied. Results demonstrate the effectiveness of the employed classification model, techniques and rules, in obtaining highly accurate (over 90%) mapping results on the spatial extent of water-related ecosystems. Also, they highlight the contribution of Earth Observation (EO) and geospatial analysis in assessments of area-based changes and their causes, as well as in identification of conservation and management priorities (i.e. areas for restoration). In addition, to address the need to strengthen national capacities, the established SWOS service lines have been used as a contribution to the user community.

1. Introduction

Water-related ecosystems play a critical role in the water cycle. Amongst them, wetland ecosystems are those in which water is the main component driving their functions and the services they provide. According to the Ramsar Convention, almost all of the world's consumption of freshwater is drawn either directly or indirectly from wetlands. They also provide services such as food, fiber and timber products, transport, recreation, and waste removal (Ramsar Convention Secretariat, 2010). Moreover, wetland ecosystems are considered essential in achieving several Sustainable Development Goals (SDGs) (Ramsar Convention Secretariat, 2018).

In accordance with the Aichi Biodiversity Targets of the Convention on Biological Diversity, by 2020, the protection and restoration of water-related ecosystems have been included in the SDG target 6.6. In particular, the proposed SDG Indicator 6.6.1 monitors change in the extent of water-related ecosystems over time, focusing in freshwater wetland ecosystems (vegetated wetlands, rivers, lakes, aquifers and artificial water bodies). Further options are suggested to expand it in non-freshwater ecosystems (i.e. mangroves, estuaries) due to relationships that may exist (UN Environment-Water, 2018). A broader conception of wetland ecosystems is adopted by the Ramsar Convention, which under the collective term "wetland ecosystems", defines a wide variety of water-related habitats, such as marshes, peatlands, floodplains, rivers and lakes, regardless of their depth, coastal areas and marine areas no deeper than six meters at low tide, as well as human-made wetlands.

* Corresponding author.
E-mail address: helenf@ekby.gr (E. Fitoka).

https://doi.org/10.1016/j.rse.2020.111795
Received 15 November 2018; Received in revised form 25 February 2020; Accepted 23 March 2020

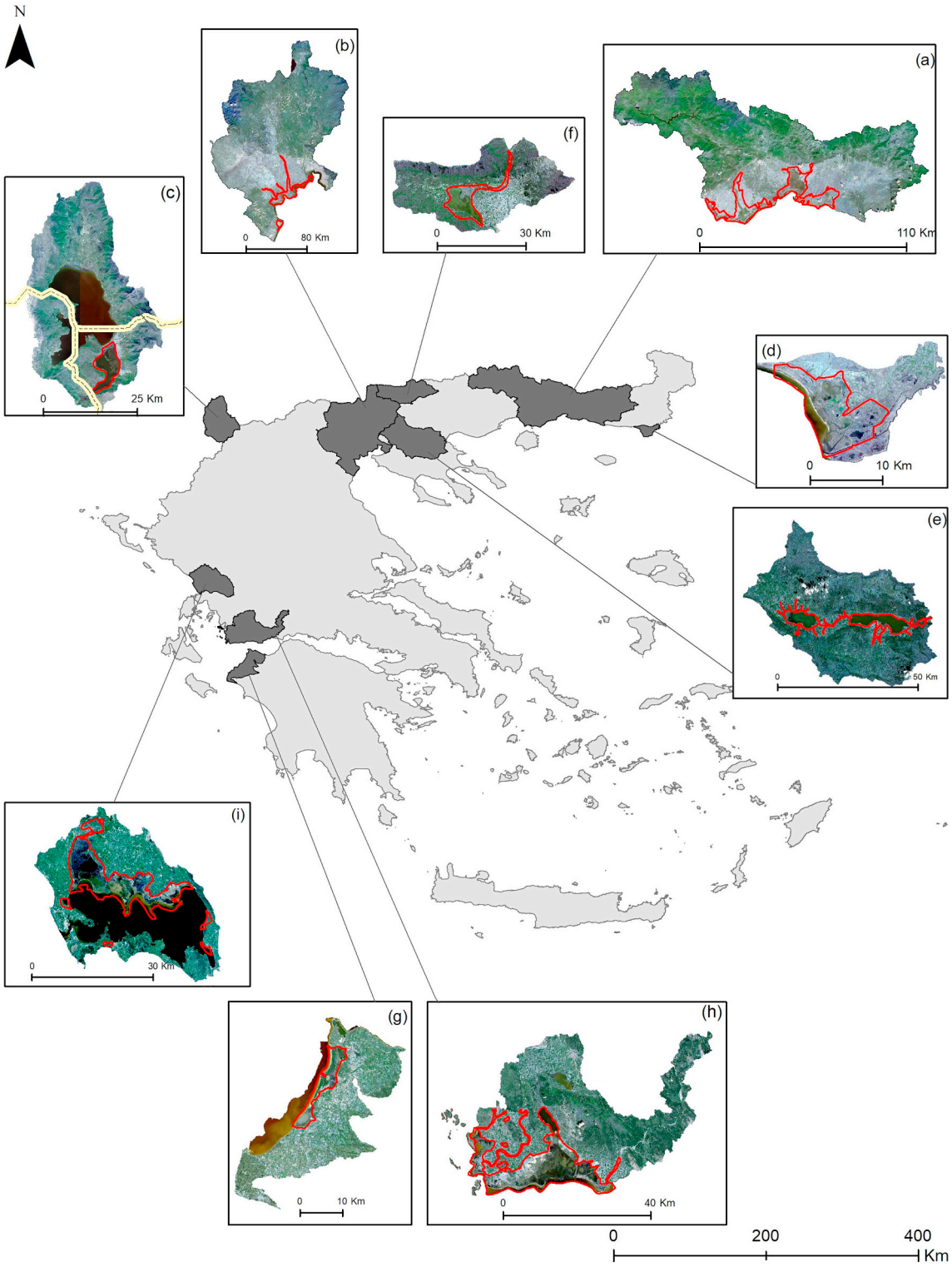

Fig. 1. Pilot areas (include Ramsar sites and their catchments)/Ramsar site codes: (a) Eastern Macedonia and Thrace National Park/GR55 (Nestos Delta) & GR56 (Vistonida Lagoon); (b) Axios, Loudias, Aliakmon Deltas/GR59; (c) Transboundary Prespa Lakes/GR60, AL2151, MK726; (d) Evros Delta/GR54; (e) Volvi and Koronia Lakes/GR57; (f) Kerkini Lake/GR58; (g) Kotychi Lagoon/GR63; (h) Messolonghi Lagoon/GR62; (i) Amvrakikos Gulf/GR61. The red polygon denotes the Ramsar site. (For interpretation of the references to colour in this figure legend, the reader is referred to the web version of this article.)

At European and regional level, the mapping of wetland ecosystems' spatial extent is a priority under various European and regional policies, treaties and initiatives. Notable are the EU Biodiversity Strategy to 2020, the EU Habitat and Birds Directives, the EU Water Framework Directive (WFD), the EU Initiative on Mapping and Assessment of Ecosystems and their Services (MAES), the EU Strategy on Green Infrastructure and the Mediterranean Wetlands Initiative. Still, due to many bottlenecks driven mainly by lack of standardization and common consensus on wetland ecosystem types, wetlands are under-represented in size and diversity, affecting conservation and restoration efforts.

Within Earth Observation (EO) technology, mapping of wetland

ecosystems' spatial extent has been proven a challenging task (Dronova et al., 2012). It is very well-suited in identifying changes, degradation, and responses to restoration, because of its synoptic repetitive coverage over the same area at various spatial and temporal scales (Perennou et al., 2018; Ballanti et al., 2017; Singh et al., 2017; Sanchez-Hernandez et al., 2007). Nevertheless, the overall success and practical utility of remote sensing-based wetland assessments have been contingent on the accuracy of image interpretation and feature extraction (Dronova, 2015). The spatial structure and composition of wetland habitats are complex with not easily distinguishable boundaries, which leads to within-class spectral variability and spectral similarities between classes as well (Keramitsoglou et al., 2015). The advent of newly launched satellites with enhanced spatial and/or spectral resolutions, along with the development of efficient algorithms can address the above challenges. In particular, Object-based Image Analysis (OBIA) offers a promising framework to address these constraints in heterogeneous landscapes and to facilitate repeated monitoring of wetland ecosystem surface properties and configuration (Dronova, 2015; Wang et al., 2004). Guo et al. (2017) and Dronova (2015) reviewed many studies that incorporated OBIA for wetland classification with various EO dataset and variables. The outcomes showed the effectiveness of OBIA, particularly via a hierarchical framework. When compared to traditional pixel-based techniques, OBIA proved superior because of the incorporation of spectral and spatio-contextual information (Blaschke, 2010; Ceccarelli et al., 2013). Further, Ma et al. (2017) reviewed many studies that applied OBIA for land-cover classification, and they found that most of the study areas were < 300 ha (95.6%). The above authors suggest the need for larger study areas in future research, thereby verifying the applicability of the object-based image classification technique over wider areas. The main objective of the current study was the mapping and assessment of the 10 Greek Ramsar wetland sites and their catchments as a contribution to knowledge for SDG 6.6.1 indicator assessment and to the update of Ramsar Information Sheets. Particularly we aimed:

- to generate a hierarchical object-based image analysis model tailored to wetland ecosystems and to identify limitations and rules in mapping their spatial extent, following the MAES ecosystem nomenclature as modified within SWOS;
- to estimate the spatial extent of wetland ecosystems of Greek Ramsar sites over their catchment areas and to assess potential changes and their causes.

2. Material and methods

2.1. Study sites

The study was carried out in the 10 Greek Ramsar sites and their catchment areas. Two of them comprise the National Park of Eastern Macedonia and Thrace, and along with their catchment areas they were treated as one continuous area. It is noted that Greek Ramsar site Prespa Lakes (GR 60) is part of the transboundary ecosystem shared by Greece, Albania and North Macedonia; as a contribution to transboundary integrated management of the area, the mapping area was extended in these countries too. The analysis was carried out in a total area of 2,015,091 ha (Fig. 1). In this work only mapping results for the Greek territory are presented (1,858,666 ha).

2.2. Datasets and pre-processing

Sentinel 2A-MSI standard level-1C (L1C) products were used, available from the Copernicus Open Access Hub website. They are distributed as ortho-rectified and UTM (Universal Transverse Mercator) geocoded Top-of-Atmosphere (TOA) reflectance images. The spatial resolution of the L1C products is 10 m, 20 m or 60 m depending on the band (Table 1) (Agency, 2018; Drusch et al., 2012). 42 Sentinel -2A MSI (S2) tiles were acquired for 2016–2017. Of these, 21 were acquired for the wet season (March to May) and 21 for the dry season (June to August) (Table 2). Cloud cover was under < 15%, thus cloud masking was not required.

Table 1
Spectral and spatial information per band of Sentinel 2A-MSI sensor (Agency, 2018) and Landsat 5TM (USGS, 2017).

Sentinel 2_MSI bands	Central wavelength (μm)	Resolution (m)
Band 1 - coastal aerosol	0.443	60
Band 2 - blue	0.490	10
Band 3 - green	0.560	10
Band 4 - red	0.665	10
Band 5 - vegetation red edge	0.705	20
Band 6 - vegetation red edge	0.740	20
Band 7 - vegetation red edge	0.783	20
Band 8 - NIR	0.842	10
Band 8A - vegetation red edge	0.865	20
Band 9 - water vapour	0.945	60
Band 10 - SWIR - cirrus	1.375	60
Band 11 - SWIR	1.610	20
Band 12 - SWIR	2.190	20

Landsat 5 TM bands	Central wavelength (μm)	Resolution (m)
Band 1 - blue	0.45–0.52	30
Band 2 - green	0.52–0.60	30
Band 3 - red	0.63–0.69	30
Band 4 - NIR	0.76–0.90	30
Band 5 - SWIR	1.55–1.75	30
Band 6 - thermal	10.40–12.50	120
Band 7 - SWIR	2.08–2.35	30

In addition, Landsat 5 TM Level 1TP products were employed, provided by the USGS, in order to map the pilot areas in the past, covering the longest possible period. These products are distributed as radiometrically calibrated and ortho-rectified using ground control points and digital elevation model data (Table 1) (USGS, 2017). In particular, 34 Landsat 5 TM (L5) images of 1985–86 were employed in this analysis, 17 for each season. The acquisition dates were carefully chosen so as to be relevant with the acquisition dates of the appropriate Sentinel 2A images per site. However, minor exceptions were permitted in some cases due to lack of available imagery. Similarly, the cloud cover was below < 10% with no cloud masking required over the selected L5 tiles.

Table 2
Acquisition dates of the imagery used per sensor and pilot area.

Pilot area name (Ramsar site and its catchment)/Ramsar site codes	Sentinel 2A-MSI (10 m)	Landsat 5TM (30 m)
(a) Eastern Macedonia and Thrace National Park/GR55 & GR56	21-Apr-16 10-Jul-16	18-May-87 22-May-86 19-Aug-86 10-Aug-86
(b) Axios, Loudias, Aliakmon Delta/GR59	04-Apr-16 02-Aug-16	24-Apr-85 17-Aug-86
(c) Transboundary Prespa Lakes/GR60, AL2151, MK726	17-Apr-16 15-Aug-16	02-Apr-86 24-Aug-86
(d) Evros Delta/GR54	04-Mar-17 26-Aug-17	16-Feb-89 24-Aug-88
(e) Volvi and Koronia Lakes/GR57	30-Mar-17 12-Aug-17	04-Apr-86 10-Aug-86
(f) Kerkini Lake/GR58	30-Mar-17 12-Aug-17	24-Apr-85 17-Aug-86
(g) Kotychi Lagoon/GR63	09-Apr-17 27-Aug-17	07-Mar-85 17-Aug-86
(h) Messolonghi Lagoons/GR62	09-Apr-17 27-Aug-17	07-Mar-85 17-Aug-86
(i) Amvrakikos Gulf/GR61	09-Apr-17 27-Aug-17	02-Apr-86 23-Jul-86
Total number of images	42 tiles	34 tiles

All satellite images were atmospherically corrected using the Semi-Automatic Classification Plugin (SCP) embedded in QGIS software (Congedo, 2016), which applies a dark object subtraction algorithm (Chavez, 1988), converting the TOA values into surface reflectance values. In the case of S2, for each tile, 10 out of 13 bands (b2-b8A and b11-b12) were stacked into a single file resampled to 10 m spatial resolution. In the end, two single 10-band layers, one for wet and one for dry season were generated, per pilot area. The same procedure was applied in the L5 images, where for each tile, the appropriate bands (b1-b5 and b7) were employed resulting in single files of 30 m spatial resolution. In the end, two single 6-band layers, one per season, were generated for each pilot area.

The Corine Landcover/Landuse (CLC) national datasets of 2012 and 2000 were used as additional thematic layers within the classification model, in order to discriminate "Croplands" (CLC codes of Level 3: 211,212,221,222,223,231,241,242 and 244) from "Urban" classes (CLC codes Level 1: 1), and from "Rice fields" classes (CLC code: 213). Even though there is a spatial and time deviation between the satellite imagery employed and the CLC layers, due to the lack of other relevant spatial datasets, the CLC 2012 was employed for the recent mapping (2016–2017) while the CLC 2000 was used for the past one (1986–1987). This was decided because croplands, which are highly dynamic, as each crop may be in a different state of development, present spectral similarities with other natural land cover categories that leads to limitations of mapping accuracies (Ozdogan et al., 2010). Similarly, challenges in discriminating accurately the urban surfaces with remote sensing exist, due to high spectral and spatial variability of urban surface materials (Powell et al., 2007). Therefore, a visual evaluation in terms of spatial coherence, was applied in the CLC datasets and further delineation was employed where needed.

2.3. Wetland spatial extent mapping approach

2.3.1. Nomenclature

Within SWOS, wetland ecosystems are considered connected with their broader landscapes in hydrological and ecological terms, and within a human context. As such, wetland ecosystems can encompass their larger surroundings, both waterscapes and landscapes, including even the non-wet habitats such as sand dune systems and beaches along coastal wetlands, or the deep water habitats of lakes, underground aquifers, and even the degraded wetlands which have significantly lost their naturalness but potentially could be restored.

The EU MAES nomenclature (https://biodiversity.europa.eu/maes/typology-of-ecosystems), as modified and enhanced within SWOS (Fitoka et al., 2017), was followed in this analysis. The classes applicable at the pilot areas (Table 2) were selected prior to image analysis, based on existing knowledge and preliminary inspection of the available images as well as of Google Earth imagery. Based on established cross walks (Fitoka et al., 2017) between the modified MAES and the CLC, second level mapping products were generated with the matched CLC classes (Table 3).

2.3.2. Hierarchical object-based image analysis

A hierarchical object-oriented approach was adopted in order to take into account the need for "nested" spatial configuration of wetland habitats (Dronova, 2015) and to have the flexibility required in wetland ecosystem mapping (Grenier et al., 2007).

For each pilot area, two single 10-band S2 images (recent time: 2016–2017) or 6-band L5 TM images (past time 1986–1987), one per season (wet and dry), were segmented by applying the multi-resolution segmentation algorithm embedded in the eCognition Developer 8.7 software (Trimble Inc.). In order to generate meaningful real-world objects of interest (Castilla and Hay, 2008), several user-defined parameters were tested through visual inspection, such as scale, colour/shape, smoothness/compactness. In particular, the scale parameter, which may directly affect subsequent classification (Smith, 2010), was iteratively assessed in order to control whether small patches of specific cover (i.e. water, bare land, grasses) should be embedded in coarser classes (i.e. coastal marshes, forests) or not. In the end, two segmentation levels were selected (Table 4).

A superset of 78 object features was compiled, that could potentially be used to discriminate the wide range of classes in all pilot areas, including spectral, geometric and contextual variables (Table 5). In particular, spectral information of both seasons was used for the calculation of spectral indices, such as the Normalized Difference Vegetation Index – NDVI (Townshend and Justice, 1986), the Normalized Difference Water Index – NDWI (McFeeters, 1996), and the Normalized Difference Red Edge Index – NDRE (only for the S2 case) (Barnes et al., 2000).

A top-down process was followed, so as to initially identify the easiest or more general classes (parent classes) (i.e. water surface, bare land, forest, permanently flooded marshes, low stature herbaceous) and then proceed with the classification of the detailed classes (child classes) to reach the 3rd or even the 4th level of MAES nomenclature (Table 3). The classification approach is a combination of user-defined rules, Classification And Regression Tree - CART Decision tree algorithm, and context-based classification. Particularly, CART was utilized alongside as a support tool offering guidance for classes that presented spectral similarities and were difficult to define. CART is a well-known decision tree classification algorithm which uses a multi-stage approach to the problem of label assignment (Breiman et al., 1984). It is considered to be a chain of simple decisions based on the results of iterative tests rather than a single complex decision (Pal and Mather, 2003). As a supervised-classifier, it requires labeled training data, thus training samples were carefully chosen, based on existing knowledge, orthophotos and Google Earth. The final result of the CART analysis, which naturally extends to a rule-based classification scheme, was manually integrated within the ruleset in order to be reasonably robust and transferable.

Subsequently, a context-based classification was applied, in order to reach classes, such as river banks, riparian broadleaved forest, wet grassland (Fig. 2), that could be effectively isolated and classified only through comparison to others. Particularly, user-defined classification rules were applied based on contextual features as described in Table 5. The use of contextual information helped to progressively quantify the relationship between an individual object and its neighbor ones, because as more objects are classified, more context information is available to classify other, less easily defined (O'Neil-Dunne and Pelletier, 2011).

The hierarchical image classification flow (Fig. 2) was generated in the pilot area of the National park of Eastern Macedonia and Thrace and its catchment area, based on the correspondent S2 dataset, and formed the fundamental set of steps that also applied to the other pilot areas. Since the objective of this analysis was the generation of mapping products of high accuracy and not the transferability of the ruleset per se, the rules behind each feature selected for the discrimination of each class, were evaluated prior to their application in each pilot area.

At the first segmentation level (coarse-scaled), the "Water surfaces" were easily defined based on the Normalized Difference Water Index – NDWI, calculated for both seasons, along with the Brightness index. It should be mentioned that in order for an object to be labeled as "Water surfaces", it had to represent a water surface in both seasons/images. Accordingly, the "Croplands", "Urban" and "Rice fields" were derived from CLC 2012.

At the second segmentation level (fine-scaled), the features that initially were employed to define the "Water surfaces", were re-applied in order to isolate smaller-scaled objects that belonged to the specific class. Geometry features, such as the size of the object under investigation or its shape, were further used to define water-related classes of the fourth level of the classification scheme. In particular, "Ponds" were discriminated based on the size of the object classified as "Water surfaces" where a general rule exists (covered area below 8 ha),

Table 3
Classes applicable in pilot areas according to the MAES nomenclature and the CLC as these have been enhanced within SWOS ("/" denotes attributes that further distinguishes some MAES classes).

MAES classes enhanced based on EUNIS & Ramsar types	CLC classes enhanced based on Ramsar types
1 Urban	1 Artificial surfaces
2 Croplands	2 Agricultural areas
2.1.3.1 Rice fields	2.1.3 Rice fields
3.1 Broadleaved forest	3.1.1 Broad-leaved forest
3.1.1 Riparian and fluvial broadleaved forest	3.1.1.2 Wet forests including riparian
3.2 Coniferous forest	3.1.2 Coniferous forest
3.2.1 Riparian and fluvial coniferous forest	3.1.2 Coniferous forest
4.1 Dry grasslands	3.2.1 Natural grassland
4.3 Wet grasslands	4.1.1.7 Seasonal/intermittent freshwater marshes/pools on inorganic soils, includes sloughs, potholes, seasonally flooded meadows, sedge marshes
5.1.1.4 Riverine and fen scrubs	3.2.4.1 Shrub-dominated wetlands, shrub swamps, shrub-dominated freshwater marshes, shrub carr, alder thicket on inorganic soils
5.2.1 Sclerophyllous vegetation/coastal dune scrub	3.2.3 Sclerophyllous vegetation
6.2 Bare soil, rock, perennial snow & ice	3.3 Open spaces with little or no vegetation
6.2.1.1 Beaches	3.3.1.1 Sand, shingle or pebble shores, includes sand bars, spits and sandy islets, includes dune systems and humid dune slacks
6.2.1.2 Coastal and fluvial dunes without vegetation	3.3.1.1 Sand, shingle or pebble shores, includes sand bars, spits and sandy islets, includes dune systems and humid dune slacks
6.2.1.3 River banks	5.1.1.2 Permanent rivers/streams/creeks, includes waterfalls
7.1.1.1 Inland freshwater marshes without reeds (small ponds below 8 ha might be included)/permanently flooded	4.1.1.6 Permanent freshwater marshes/pools, ponds (below 8 ha), marshes and swamps on inorganic soils, with emergent vegetation water-logged for at least most of the growing season
7.1.1.1 Inland freshwater marshes without reeds (small ponds below 8 ha might be included)/seasonally flooded	4.1.1.7 Seasonal/intermittent freshwater marshes/pools on inorganic soils, includes sloughs, potholes, seasonally flooded meadows, sedge marshes
7.1.1.2 Inland freshwater marshes with reeds (small ponds below 8 ha might be included)	4.1.1.1 Reedbeds and high helophytes
8.1.1 Salt marshes without reeds/permanently flooded	4.2.1 Salt marshes
8.1.1 Salt marshes without reeds/permanently flooded/seasonally flooded	4.2.1 Salt marshes
8.1.2 Salt marshes with reeds	4.2.1 Salt marshes
8.2.1 Coastal lagoons	5.2.1.1 Coastal brackish/saline lagoons, brackish to saline lagoons with at least one relatively narrow connection to the sea
8.2.2 River estuaries and estuarine waters of deltas	5.2.2 Estuaries
8.3.1 Coastal saltpans (highly artificial salinas)	4.2.2 Salines
8.4.1 Intertidal flats	4.2.3.1 Intertidal mud, sand or salt flats
9.1.1.1 Permanent Interconnected running water courses	5.1.1.2 Permanent rivers/streams/creeks, includes waterfalls
9.1.1.3 Highly modified natural water courses and canals	5.1.1.4 Canals and drainage channels, ditches
9.2.1.1 Natural permanent water bodies (over 8 ha)	5.1.2.1 Permanent freshwater lakes (over 8 ha), includes large oxbow lakes
9.2.2.1 Ponds and lakes with completely man-made structure (generally below 8 ha)	5.1.2.10 Ponds, includes farm ponds, stock ponds, small tanks, (generally below 8 ha)
9.2.2.4 Other reservoirs/barrages/dams/impoundments etc. (generally over 8 ha)	5.1.2.11 Water storage areas, reservoirs/barrages/dams/impoundments (generally over 8 ha)
10.1.1 Marine waters less than six meters deep at low tide	5.2.3.1 Permanent shallow marine waters in most cases less than six meters deep at low tide, includes sea bays and straits

Table 4
User-defined segmentation parameters per sensor and segmentation level.

Segmentation levels	Sentinel 2-MSI	Landsat 5 TM
Level 1 (coarse)	Image layers weighted: All spectral information images of both seasons Thematic layer used: CLC layer Scale: 150 Shape: 0.3 Compactness: 0.7	Image layers weighted: All spectral information images of both seasons Thematic layer used: CLC layer Scale: 400 Shape: 0.1 Compactness: 0.5
Level 2 (fine)	Image layers weighted: All spectral information images of both seasons Thematic layer used: None Scale: 60 Shape: 0.7 Compactness: 0.5	Image layers weighted: All spectral information images of both seasons Thematic layer used: None Scale: 100 Shape: 0.3 Compactness: 0.5

while extent features (i.e. length, length/width) and shape features (i.e. roundness) were used for the discrimination of the "Permanent interconnected running waters".

Furthermore, certain contextual features, such as "distance from", "border to" and "relative border to", were chosen for the re-classification of objects next to objects or spatially relevant to objects already classified in wetland classes (Fig. 2). For example, the "Riparian broadleaved" class was defined by objects already classified as "Broadleaved forest" that were next to objects of certain wetland-related classes (i.e. rivers, river banks). The distance from "Marine water" was used in order to differentiate the inland marshes from the coastal salt marshes.

As previously mentioned, the classification ruleset was adjusted in each pilot area, since the aim of the analysis was driven by the user needs for highly accurate products. Particularly, three different cases of adjustments were made. The first one related to those classes (parent and child) that their spectral-based features were constant in all pilots, although their respective range of values, set in one pilot, was re-adjusted for a better classification result in another pilot. Classes of this case, are the "Water surfaces" (parent class) and its respective child

Table 5
List of object features divided into four categories according to eCognition 's categorization; (ds) and (ws) denote features derived from dry season and wet season images, respectively.

Feature categories	Features	Description	Number of features
Customized (Spectral indices)	NDVI (ws, ds)	$NDVI = \frac{NIR - RED}{NIR + RED}$	7
	NDWI (ws, ds)	$NDWI = \frac{GREEN - RED}{GREEN + RED}$	
	NDRE (ws, ds)	$NDRE = \frac{NIR - \mathrm{Re}\,dEdge}{NIR + \mathrm{Re}\,dEdge}$	
	Ratio of NDWI (ds)/(ws)		
Layer values (Spectral Features)	Mean (for all image layers both ds and ws)	The mean value represents the mean brightness of an image object within a single band	42
	Brightness	Sum of mean values in all bands divided by the number of bands.	
	Max. difference	Minimum mean value of an object subtracted from its maximum value. The means of all bands belonging to an object are compared with each other. Subsequently, the result is divided by the brightness	
	Standard Deviation (for all image layers both ds and ws)	The standard deviation of all pixels which form an image object within a band	
Geometry	Extent	Area, Border length, Length/Width	3
	Shape	Compactness, Roundness	2
Thematic attributes	CLC thematic layer	Croplands, Rice fields, Urban	3
Class-related (Contextual features)	Relations to super objects	Existence to "Water Surfaces"	1
	Relation to neighbor objects	Border to, Relative border to features. These contextual features were applied to all spectral-based defined classes that further discriminated into detailed classes (total 8 classes). Distance to feature. This was employed in order to discriminate the coastal from the inland correspondent categories. (Fig. 2)	20
Total			78

classes ("Marine water", "Coastal lagoon", "Inland water"), the "Marsh permanently flooded" (with and without reeds), the "Broadleaved forest" and the "Intertidal flats".

The second case related to classes that their selected spectral features differed from pilot to pilot. Particularly, those that presented high spectral similarities with others (i.e. Coniferous forest with Sclerophyllous vegetation), or a class in one pilot differed from the other, i.e. "Rivers" due to differences in water recharge volumes; "Dry grassland" due to differences in vegetation coverage, when it was sparse they were confused with the "Bare land" while in others they were easily distinguished. Moreover, regarding the water-related classes, it has been observed that the appropriate features had to be changed when the number of water child classes was different between the pilot sites (i.e. existence of rivers and lagoons and marine waters in one site or existence of only one class in another one).

The third case of adjustments referred to the contextual–defined classes, where the values of the respective feature were changed prior to their application in each pilot. The lack of general contextual criteria is reasonable while values of some ecologically driven parameters (i.e. extent of riparian zone, extent of soil moisture) are site-specific and require additional knowledge on climatic and topographic conditions. To overcome this bottleneck, an iterative internal evaluation was undertaken in order to define contextual classes per site, as was the case of the distance next to "River" or "River bank" that "Riparian broadleaved forest" extents.

Similarly, the "Marsh without reeds seasonally flooded" (coastal and inland) class, which was difficult to identify in most sites, was isolated based on contextual features which were adjusted at each pilot. This class presented spectral differentiation between the two seasons, that was fused with other classes. For the wet season, this class was spectrally similar to grasslands due to the fact that both are dominated by low statute herbaceous vegetation (parent class), while for the dry season it presents sparse vegetation, a situation that was spectrally fused with "Bare land". By applying the appropriate contextual features, when objects defined as "Low stature herbaceous" and/or "Bare land" were next to wetland classes, these were further classified as "Marsh without reeds seasonally flooded". Moreover, the lack of spectral features possible to define the specific class, generated discrimination issues between "Wet grassland" and "Dry grassland". To overcome these difficulties, expert-knowledge rules were applied which suggested that permanently flooded marshes are usually followed by seasonal flooded marshes which extent towards the upland side and that wet grasslands are usually found next to water bodies (i.e. rivers, lakes) where water fluctuations occur.

2.4. Thematic accuracy assessment

The accuracy assessment was applied in a sample area covering 66% of the total mapped area including 5 out of the 10 Greek Ramsar sites and all possible wetland classes. Since reference data for the previous years (1986) were not available, the accuracy assessment was only applied in the classification products of the recent dates (2016–2017). It consisted of three fundamental steps: the determination of the appropriate sample size, the sampling design and the specification of the appropriate measure of accuracy (Foody, 2002). Multinomial distribution was used to determine the sample size, since multiple classes compose the final thematic products (Congalton and Green, 2009). The total number of point-samples (1532 points) was derived by the Eq. (1) (Table 6) introduced by Tortora (1978) (Table 7).

For the spatial distribution of the generated points, the stratified random sampling was selected, so as to ensure that all classes, no matter how small, would be included in the accuracy assessment. Segments (from the fine-scaled level) that included the spatial located point-samples, were used as a buffer-zone around each point. The appropriate class was assigned to each point based on existing knowledge and photointerpretation of ortho-rectified aerial photos (acquired on 2007–2009) and Google Earth (2012-present). The confusion matrix method was used to derive all necessary accuracy measures.

2.5. Assessment of changes in wetland spatial extent

The assessment of changes in wetland spatial extent and their causes covered a period of 30 years, the longest period with available historical images for the pilot areas. It was employed based on the second level mapping products generated with the CLC classes (Table 3) for the recent (2016–2017) and past years (1986–1987), by applying the Land

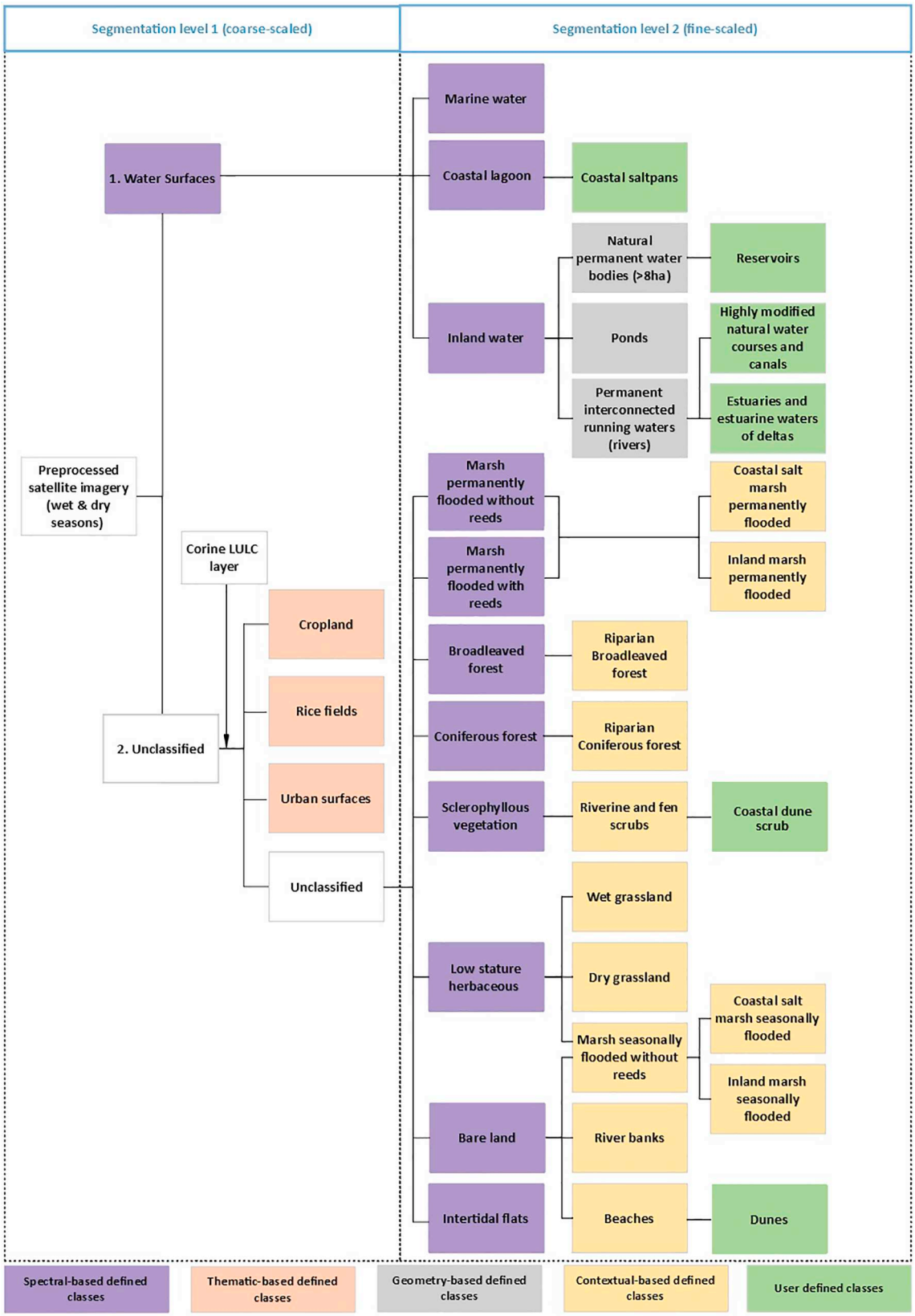

Fig. 2. Image hierarchical classification flow. The links between the classes denote the relationship between them. The classes have been defined based on their spectral characteristics (purple), geometry (grey) and with the employment of contextual features (yellow). Nevertheless, all child classes defined by contextual or geometry features, inherited the particular rules by their respective parent classes. Certain categories that presented identical spectral characteristics and no contextual linkage, were isolated manually (green). "Croplands", "Urban" and the "Rice fields" were identified by using the CLC thematic layers (orange). (For interpretation of the references to colour in this figure legend, the reader is referred to the web version of this article.)

Table 6
Mathematical equation for sample size calculation.

(1)	$N = \frac{[B\Pi i(1-\Pi i)]}{b_i^2}$	Πi is the proportion of a population in the ith class out of k classes that has the proportion closest to 50% bi is the desired precision (e.g., 5%) for this class B is the upper (a/k) × 100th percentile of the chi square (×2) distribution with 1 degree of freedom k is the number of classes

and Ecosystem Accounting – LEAC classification of land cover changes in Land Cover Flows (LCF) (European Environment Agency, 2006) (supplementary material).

A map-to-map comparison approach was selected (Singh, 1989) due to spectral similarities that many wetland classes presented, particularly those defined by contextual features or geometry characteristics. Problems occurred by the mis-registration of the polygons boundaries (different pixel value and/or misclassifications in one or both maps) and resolved through a post-processing of the spatial overlay analysis result (i.e. elimination of polygons under 0.3 ha).

3. Results - discussion

3.1. Hierarchical image classification model

The implementation of the hierarchical object-oriented classification flow in the analysis of the S2 images, resulted in the discrimination of 31 classes of the modified MAES typology, of which 24 corresponded to wetland ecosystems. The analysis highlighted the need for seasonal spectral information for the discrimination of several wetland classes while the utility of geometric and contextual criteria was essential in order to reach the detailed 3rd and 4th levels of the nomenclature (Fig. 3).

A combination of NDWI and Brightness index ranges of values was employed to discern the “Marine water” from the “Coastal lagoon”. Nevertheless, some specific water-related classes were not possible to be successfully isolated using spectral and/or contextual features. Thus, the assignment of the class was applied manually based on existing knowledge of the area i.e. “Reservoirs”. Different ranges of NDWI values (calculated for both seasons) were used for the classification of the “Marshes (with and without reeds) permanently flooded”. Due to water permanency throughout most of the year and due to the phenological seasonal differences of the persistent emergent vegetation, the relevant objects presented a special spectral differentiation.

Moreover, in the case of S2, the existence of available information within the spectrum range of 0.705–0.865 μm, for both seasons (wet and dry), assisted in defining other classes which present seasonal differences due to changes in vegetation phenology (such as the “Broadleaved forest” and the “Low stature herbaceous”) or in water level fluctuations (such as “Intertidal flats”). The mean values of SWIR -1 and -2 bands (1.610–2.190 μm) were used to define the “Coniferous forest” class since the SWIR reflectance for coniferous is low compared to the broadleaves (Rautiainen et al., 2018)

Both red-edge and SWIR bands from Sentinel-2 were important, confirming that seasonal images can capture phenological differences between the species (Persson et al., 2018). On the other side of the spectrum range, the mean values of the Blue bands (0.490 μm) formed the basic features for the discrimination of the “Bare land” class. The particular class presented less spectral variation in comparison with the vegetated ones. This is due to factors, such as soil texture, surface roughness and organic matter, that affect soil reflectance acting over less specific spectral bands (Govender et al., 2007). A similar approach was adopted in the case of L5 imagery, where features from the spectrum ranges closest to the S2 were used.

3.2. Thematic accuracies

The Overall Accuracies (OA) showed that the classification flow exhibited satisfactory results in terms of overall performance and kappa coefficient (Table 8). Some errors were rather expected and to some level were related with the bulk delimitation of the “Cropland” and “Urban” from CLC2012 which did not temporarily coincide with the image acquisition dates. Thus, possible croplands not covered by CLC2012, were classified in most of the cases as “Dry grassland” or “Bare” according to their spectral behavior, explaining the medium User's Accuracy (UA) of them. Further, in the cases where the applied contextual criteria concerned these two classes, their omission errors might have been transferred in classes “Wet grassland” or “Marsh seasonally flooded” respectively. However, worthy to note is that in many cases, these omission errors highlighted a rather common situation, that of the seasonal expansion of crops against wetland extent. With regard to nature conservation and restoration needs, although these areas do not have dominant wetland characteristics, they are considered as degraded wetland ecosystems and it is suggested that they are included in the total wetland extent calculation.

Moreover, the high accuracies of classes that were defined based on spectral and contextual features (i.e. “Coastal salt marshes permanently flooded”) demonstrate the effectiveness of the combined classification approach. However, the success of UA of certain categories defined by contextual criteria (i.e. “Riparian broadleaved forest”) with their concurrent medium PA, underlines the subjectivity presented when contextual features are employed (Li et al., 2014). Such results can become useful for updating the distance rule. It should be mentioned that in the case of “Riparian coniferous forest”, the area covered was very small leading to low accuracy results.

3.3. Wetland spatial extent within catchments and within the Greek Ramsar sites

For the recent years (2016–2017), within the catchment areas of the 10 Greek Ramsar sites (1,858,666 ha), the total wetland spatial extent reached 178,912 ha. Its highest proportion (68%) was included within the boundaries of the designated Ramsar sites representing the 73% of the designated area, whereas the remaining area was mainly dominated by croplands. A remarkable spatial extent of inland wetland ecosystems (natural lakes, wet grasslands, freshwater marshes, riverine and fen scrubs) was found outside Ramsar sites. These areas are hydro-ecologically connected with the designated part of wetland ecosystems and

Table 7
Number of points used in the accuracy assessment procedure per pilot area.

Pilot area	Sample area (ha)	Number of thematic classes	Number of point-samples
National Park of Eastern Macedonia and Thrace (2 Ramsar sites)	95,678	20	340
Axios, Loudias, Aliakmonas Delta	512,590	29	482
Prespa Lakes	136,485	11	330
Evros Delta	21,216	17	380

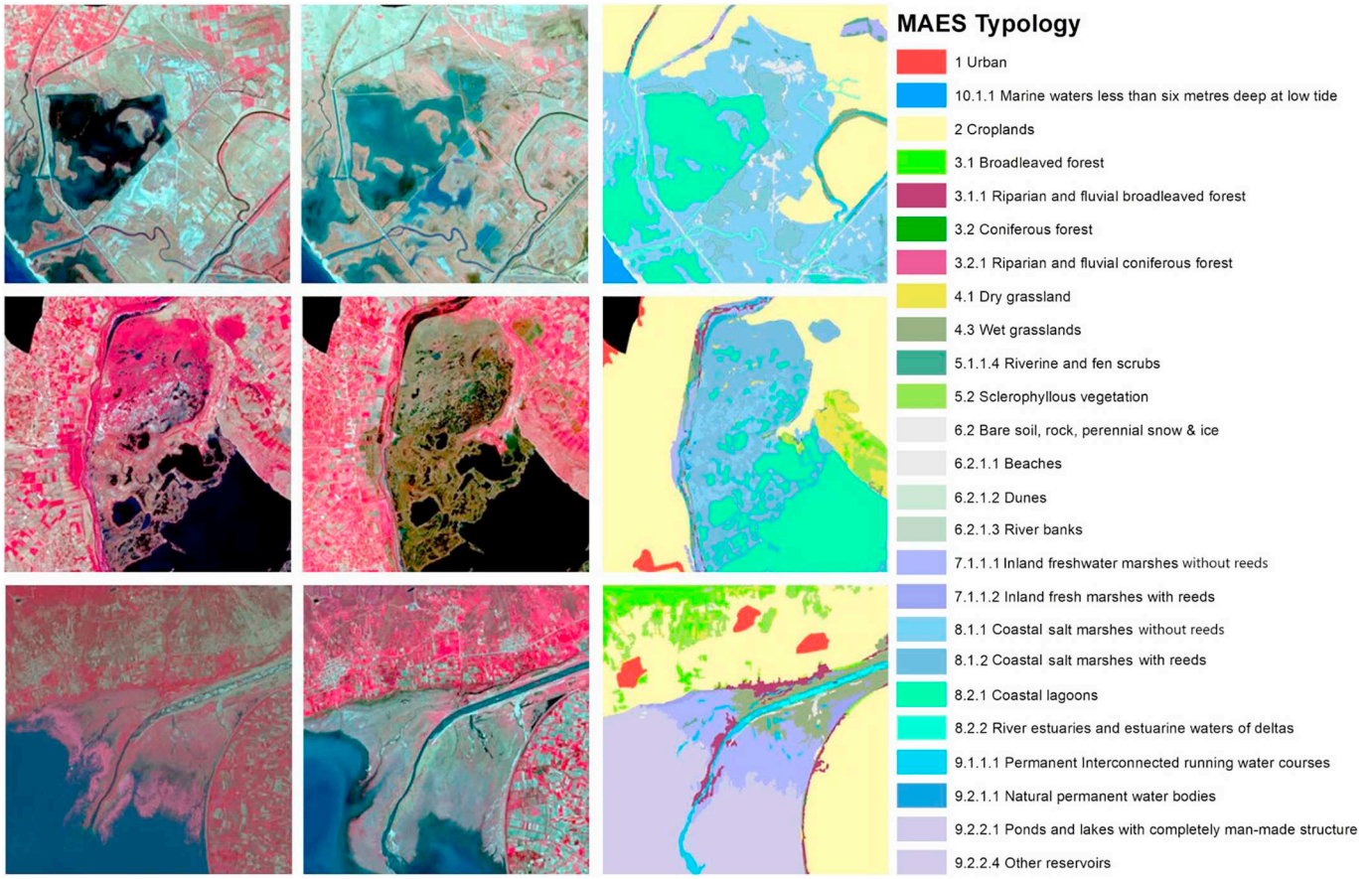

Fig. 3. Examples of classification results. The first two columns indicate the Sentinel 2A-MSI images for dry and wet season respectively; the classification result is based on modified MAES typology. The first row of pictures demonstrates the particular wetland region of Evros delta, with the "Coastal salt marsh permanently flooded without reeds" and "Coastal lagoons" being the dominant classes. The second row shows the classification of the "Coastal salt marsh with reeds" in the Amvrakikos Gulf and the characteristic spectral differentiation that this class presents between seasons. The third row demonstrates the distinctive zone of "Wet grasslands" next to the "Inland freshwater marsh without reeds" in the Kerkini Lake.

require similar management and conservation measures. Similarly, coastal wetland ecosystems (coastal lagoons, salt marshes, river estuaries and estuarine waters of deltas, beaches and coastal dunes, and intertidal flats) were located outside Ramsar sites and could be considered for inclusion in future extension of Ramsar boundaries. The rarest water-related type was that of coastal dunes scrub identified only in Axios, Loudias, and Aliakmon Delta. A significant area of the spatial extent of man-made water bodies was found within designated boundaries, and in particular, in the Kerkini Reservoir Ramsar site. For the past years (1986–1987), the total wetland extent was slightly larger, mainly due to higher wetland extent outside the designated Ramsar sites. On the contrary, within Ramsar sites, there was a recent increase in wetland extent was observed, indicating the effectiveness of conservation measures. Relevant figures with spatial extent statistics are provided in the supplementary material.

The image classification results can be further processed in order to extract new datasets meaningful in management and conservation. Very relevant is the assessment of land degradation as a major element related to the loss of biodiversity and ecosystem services. Pattern landscape analysis can be applied to identify human–natural interface zones (Riiters et al., 2010). Fig. 4 illustrates such an approach for a subarea of the "Eastern Macedonia and Thrace National Park" pilot. Priority areas for conservation and restoration are revealed i.e. wetland ecosystems of branches of rivers (Fig. 4b) which in the land degradation pattern (Fig. 4c) disappear from natural or mostly natural domination.

3.4. Changes in the wetland spatial extent

Computing changes in wetland extent, from years 1986–1987 to years 2016–2017, revealed both gains and losses as a result of human activities, management practices as well as natural succession processes. Total changes in spatial extent, per land cover flow type (LCF code), for all pilot areas are presented in Table 9.

3.5. Potential contributions to users and reporting obligations

The need to strengthen national capacities in reporting mechanisms as well as to make data and information accessible is widely recognized by conventions and initiatives (i.e. Convention on Biological Diversity, Ramsar Convention, EU MAES Imitative, SDGs). With regard to SDG 6.6.1 indicator, its methodology piloting phase revealed significant capacity challenges in monitoring and reporting the changes within water-related ecosystems; it was concluded that the technical and institutional capacity is often lacking (UN Environment-Water, 2018). The current study contributed to the above by developing and applying a satellite based classification flow to quantify the spatial extent of different types of wetland ecosystems, their changes and causes. Furthermore, the benefits from the current study through the SWOS service lines are: (i) The image analysis results for the 10 Greek Ramsar sites, are available through the SWOS/GEOWetland community portal

Table 8
Statistical accuracy measures calculated separately for four pilots (PA stands for Producer's Accuracy and UA for User's Accuracy; empty cells indicate the correspondent categories that were not present in the respective pilot).

MAES classes	National Park of Eastern Macedonia and Thrace (2 Ramsar sites)		Axios, Loudias, Aliakmonas Delta		Prespa Lakes		Evros Delta	
	2016		2016		2017		2017	
	PA	UA	PA	UA	PA	UA	PA	UA
1 Urban	100.00%	100.00%	94.12%	100.00%	100.00%	100.00%	80.00%	100.00%
10.1.1 Marine waters less than six metres deep at low tide	100.00%	100.00%	100.00%	100.00%			100.00%	100.00%
2 Croplands	100.00%	100.00%	100.00%	100.00%	100.00%	100.00%	100.00%	100.00%
3.1 Broadleaved forest	100.00%	85.71%	90.00%	96.43%	88.31%	90.67%		
3.1.1 Riparian and fluvial broadleaved forest	78.57%	100.00%	53.33%	88.89%	100.00%	80.00%	90.91%	100.00%
3.2 Coniferous forest	80.00%	71.43%	100.00%	100.00%	90.00%	100.00%		
3.2.1 Riparian and fluvial coniferous forest	0.00%	50.00%	0.00%	0.00%				
4.1 Dry grassland	71.43%	72.73%	81.82%	100.00%	87.50%	84.48%		
4.3 Wet grasslands	83.33%	90.00%	80.00%	85.71%	100.00%	100.00%	90.00%	75.00%
5.1.1.4 Riverine and fen scrubs	100.00%	88.89%	77.78%	77.78%			75.86%	88.00%
5.2 Sclerophyllous vegetation	60.00%	87.50%	92.86%	81.25%	74.29%	78.79%		
6.2 Bare soil, rock, perennial snow & ice	100.00%	100.00%	75.00%	60.00%	100.00%	80.00%	100.00%	77.78%
6.2.1.1 Beaches	100.00%	100.00%	100.00%	90.00%	100.00%	90.00%	100.00%	88.89%
6.2.1.2 Dunes							100.00%	100.00%
6.2.1.3 River banks	100.00%	100.00%	90.00%	100.00%			100.00%	100.00%
7.1.1.1 Inland freshwater marshes without reeds permanently flooded			100.00%	100.00%			100	100.00%
7.1.1.1 Inland freshwater marshes without reeds seasonally flooded			100.00%	100.00%			83.34	55.55%
7.1.1.2 Inland fresh marshes with reeds permanently flooded			91.67%	100.00%	84.62%	100.00%		
8.1.1 Coastal salt marshes without reeds permanently flooded	93.94%	100.00%	100.00%	100.00%			90.74%	94.23%
8.1.1 Coastal salt marshes without reeds seasonally flooded	90.90%	90.90%	100.00%	85.71%			97.36%	86.05%
8.1.2 Salt marshes with reeds permanently flooded			100.00%	100.00%			88.89%	100.00%
8.2.1 Coastal lagoons	100.00%	100.00%	100.00%	100.00%			100.00%	100.00%
8.2.2 River estuaries and estuarine waters of deltas	100.00%	100.00%	100.00%	100.00%			100.00%	100.00%
8.4.1 Intertidal flats			100.00%	100.00%			90.00%	100.00%
9.1.1.1 Permanent Interconnected running water courses	100.00%	100.00%	100.00%	100.00%			90.91%	100.00%
9.2.1.1 Natural permanent water bodies	100.00%	100.00%	100.00%	100.00%	100.00%	100.00%		
9.2.2.4 Other reservoirs	100.00%	100.00%	100.00%	100.00%				
Overall Accuracy (OA)	95.48%		95.44%		91.52%		94.21%	
Kappa index of Agreement (KIA)	0.9470		0.9423		0.9017		0.9354	

(https://www.swos-service.eu/swos-portal); (ii) SWOS training seminars have been offered to representatives from the Greek Ministry of Environment and from Management bodies of the Ramsar sites, to update the Ramsar Information Sheets, to continue monitoring the SDG 6.6.1 indicator, and to make use of the study results in assessments relevant to EU priorities. (iii) Wetland class discrimination findings can support further developments of the freely-available SWOS software (https://www.swos-service.eu/documents_mapping-software/).

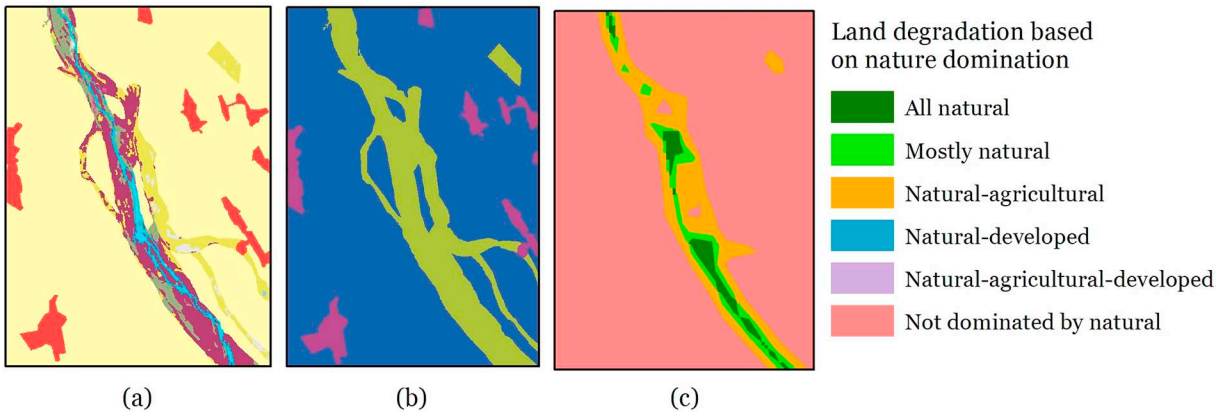

Fig. 4. Land degradation assessment. (a) image classification results; (b) reclassification in natural (green), developed-urban (magenta) and agricultural areas (blue); (c) land degradation units portraying landscape patterns of agricultural, developed and natural areas domination, performed using the GuidosToolbox (v. 2.6) software (Vogt and Riitters, 2017). (For interpretation of the references to colour in this figure legend, the reader is referred to the web version of this article.)

Table 9
Total spatial extent changes per land cover flow type (LCF code) for the 30-year time period from 1986 to 1987 to 2016–2017 (see the supplementary material for full LCF description).

LCF Code	LCF description	Area(ha)
LCF10002003	Urban sprawl	14,044
LCF221	Urban diffuse residential sprawl against wetlands	52
LCF5	Conversion from forested and natural land to agriculture	22,264
LCF52	Conversion from semi-natural land to agriculture	14
LCF521	Intensive conversion from semi-natural land to agriculture	65
LCF53	Conversion from wetlands and waters to agriculture	2241
LCF54	Conversion from developed areas to agriculture	528
LCF61	Withdrawal of farming with woodland creation	1805
LCF62	Withdrawal of farming without significant woodland creation	3790
LCF10063009	Withdrawal of farming in favor of wetlands and waters, natural changes	1745
LCF63	Farmland abandonment in favor of wetlands and waters	1659
LCF72	Forest creation, afforestation	57,410
LCF721	Forest creation, afforestation on all previously wetlands and waters	846
LCF73	Forests internal conversions	3910
LCF74	Recent felling and transition	21,336
LCF10081009	Water bodies creation AND/OR natural changes	12
LCF81	Water bodies creation (dams and reservoirs)	2018
LCF9	Changes due to natural and multiple causes	7291
LCF91	Semi-natural creation and rotation	5170
LCF911	Semi-natural creation: Natural colonization of land used by human activities	325
LCF912	Semi-natural rotation	65,132
LCF9121	Wetland and waters rotation	40,753
LCF9122	Wetland creation in dry semi-natural and natural land	3650
LCF9123	Wetland uptake from dry semi-natural and natural land	3255
LCF913	Extension of water courses	1502
LCF93	Coastal erosion	5765
LCF99	Other changes and unknown	2390

4. Conclusions

The current study, undertaken in the context of SWOS, was carried out for all 10 Greek Ramsar sites and their catchment areas (almost 17% of the inland Greek territory). It succeeded to generate a national application for mapping and assessing wetland ecosystems' spatial extent within and out of the Ramsar site boundaries (121,307 ha and 57,595 ha respectively). The MAES nomenclature, as enhanced within SWOS, proved applicable to reflect the complex spatial structure and composition of Mediterranean wetlands. Following a hierarchical object based approach, 42 Sentinel 2A-MSI images (2016–2017) and 34 Landsat 5TM images (1986–1987), covering two seasons (wet and dry), were processed. Several RS techniques were applied as well as expert – knowledge rules, ending up in the discrimination of 31 MAES classes, of which 24 corresponded to wetland ecosystems. Classification ruleset adjustments were proven necessary in order to achieve high accuracies. These, along with the generated classification flow, form potential guidance for wetland ecosystem mapping. As next steps, the enhancement of the classification model could be investigated by incorporating multi-seasonal satellite data to reveal additional phenological differences between wetland classes (i.e. marsh seasonally flooded and wet grasslands in winter) and by introducing ancillary data (topographical data).

The mapping of all ecosystem types at the entire catchments, enabled us to capture the changes in wetland extent along with their causes (i.e. conversion to agriculture). These results provide a knowledge basis for national and regional authorities of the Ramsar sites, National Parks and water districts, to identify areas for conservation and restoration and to direct sustainable management of water, natural, and agricultural resources within a hydro-ecological perspective.

The SWOS service lines provide a comprehensive user-oriented solution to improve knowledge and capacities for wetland ecosystems assessments. These, along with the shift to open-access policy in provision and employment of standard current and archive satellite data, allow the consideration for future transferability of the current national SWOS service case, in support of the SDG 6.6.1 indicator monitoring, the update of the Ramsar Information Sheets, and the implementation of the EU MAES Initiative.

Acknowledgments

This research work is funded by the European Union's Horizon 2020 research and innovation program within the Satellite-based Wetland Observation Service (SWOS) project (No 642088).

Appendix A. Supplementary data

Supplementary data to this article can be found online at https://doi.org/10.1016/j.rse.2020.111795.

References

Agency, E.S, 2018. Sentinel 2-MSI Specifications. https://sentinel.esa.int/web/sentinel/document-library/content/-/article/sentinel-2-level-1-to-level-1c-product-specifications.

Ballanti, L., Byrd, K.B., Woo, I., Ellings, C., 2017. Remote sensing for wetland mapping and historical change detection at the Nisqually River Delta. Sustainability 9, 1–32. https://doi.org/10.3390/su9111919).

Barnes, E.M., Clarke, T.R., Richards, S.E., Colaizzi, P.D., Haberland, J., Kostrzewski, M., Waller, P., Choi, C., Riley, E., Thompson, T., Lascano, R.J., Li, H., Moran, M.S., 2000. Coincident detection of crop water stress, nitrogen status and canopy density using ground-based multispectral data. In: Proceedings of the Fifth International Conference on Precision Agriculture. American Society of Agronomy, Madison, pp. 1–15.

Blaschke, T., 2010. Object based image analysis for remote sensing. ISPRS J. Photogramm. Remote Sens. 65 (1), 2–16. https://doi.org/10.1016/j.isprsjprs.2009.06.004.

Breiman, L., Friedman, J., Ohlsen, R., Stone, C., 1984. Classification and Regression Trees. Wadsworth International Group.

Castilla, G., Hay, G.J., 2008. Image objects and geographic objects. In: Blaschke, T., Lang, S., Hay, G.J. (Eds.), Object-Based Image Analysis: Spatial Concepts for Knowledge-Driven Remote Sensing Applications. Springer Berlin Heidelberg, Berlin, Heidelberg, pp. 91–110. https://doi.org/10.1007/978-3-540-77058-9_5).

Ceccarelli, T., Smiraglia, D., Bajocco, S., Rinaldo, S., de Angelis, A., Salvati, L., Perini, L., 2013. Land cover data from Landsat single-date imagery: an approach integrating pixel-based and object-based classifiers. European Journal of Remote Sensing 46 (1), 699–717. https://doi.org/10.5721/EuJRS20134641.

Chavez, P.S., 1988. An improved dark-object subtraction technique for atmospheric scattering correction multispectral data. Remote Sens. Environ. 24, 459–479.

Congalton, R., Green, K., 2009. Assessing the Accuracy of Remotely Sensed Data: Princples and Practices. CRC Press.

Congedo, L., 2016. Semi-Automatic Classification Plugin Documentation. Release 6.0.1.1. https://doi.org/10.13140/RG.2.2.29474.02242/1.

Dronova, I., 2015. Object-based image analysis in wetland research: a review. Remote Sens. 7, 6380. https://doi.org/10.3390/rs70506380.

Dronova, I., Gong, P., Clinton, N.E., Wang, L., Fu, W., Qi, S., Liu, Y., 2012. Landscape analysis of wetland plant functional types: the effects of image segmentation scale, vegetation classes and classification methods. Remote Sens. Environ. 127, 357–369. https://doi.org/10.1016/j.rse.2012.09.018.

Drusch, M., Del Bello, U., Carlier, S., Colin, O., Fernandez, V., Gascon, F., Hoersch, B., Isola, C., Laberinti, P., Martimort, P., Meygret, A., Spoto, F., Sy, O., Marchese, F., Bargellini, P., 2012. Sentinel-2: ESA's optical high-resolution mission for GMES operational services. Remote Sens. Environ. 120, 25–36. https://doi.org/10.1016/j.rse.2011.11.026.

European Environment Agency, 2006. Land Accounts for Europe 1990–2000. Towards Integrated Land and Ecosystem Accounting. EEA Report / No 11.

Fitoka, E., Poulis, G., Perennou, C., Thulin, S., Abdul Malak, D., Franke, J., Guelmani, A., Schröder, C., Zervas, D., 2017. The Wetland Ecosystems in MAES Nomenclature: SWOS Modifications (V.1.4). SWOS Technical Publication. https://www.swos-service.eu/publications/.

Foody, G.M., 2002. Status of land cover classification accuracy assessment. Remote Sens. Environ. 80, 185–201. https://doi.org/10.1016/s0034-4257(01)00295-4.

Govender, M., Chetty, K., Bulcock, H., 2007. A review of hyperspectral remote sensing and its application in vegetation and water resource studies. Water SA 33. https://doi.org/10.4314/wsa.v33i2.49049.

Grenier, M., Demers, A.-M., Labrecque, S., Benoit, M., Fournier, R.A., Drolet, B., 2007. An object-based method to map wetland using RADARSAT-1 and Landsat ETM images: test case on two sites in Quebec, Canada. Can. J. Remote. Sens. 33, S28–S45. https://doi.org/10.5589/m07-048.

Guo, M., Li, J., Sheng, C., Xu, J., Wu, L., 2017. A review of wetland remote sensing.

Sensors (Basel) 17 (4), 777. Published 2017 Apr 5. https://doi.org/10.3390/s17040777.
Keramitsoglou, I., Stratoulias, D., Fitoka, E., Kontoes, C., Sifakis, N., 2015. A transferability study of the kernel-based reclassification algorithm for habitat delineation. Int. J. Appl. Earth Obs. Geoinf. 37, 38–47. https://doi.org/10.1016/j.jag.2014.11.002.
Li, M., Zang, S., Zhang, B., Li, S., Wu, C., 2014. A Review of Remote Sensing Image Classification Techniques: the Role of Spatio-contextual Information. Eur. J. Remote Sens. 47, 389–411.
Ma, Lei, Li, Manchun, Ma, Xiaoxue, Cheng, Liang, Du, Peijun, Liu, Yongxue, 2017. A review of supervised object-based land-cover image classification. ISPRS J. Photogramm. Remote Sens. 130, 277–293. https://doi.org/10.1016/j.isprsjprs.2017.06.001.
McFeeters, S.K., 1996. The use of the normalized difference water index (NDWI) in the delineation of open water features. Int. J. Remote Sens. 17, 1425–1432. https://doi.org/10.1080/01431169608948714.
O'Neil-Dunne .S., J.M., Pelletier, K.C., 2011. Incorporating contextual information into object-based image analysis workflows. In: ASPRS Annual Conference, Milwaukee.
Ozdogan, M., Yang, Y., Allez, G., Cervantes, C., 2010. Remote sensing of irrigated agriculture: opportunities and challenges. Remote Sens. 2, 2274. https://doi.org/10.3390/rs2092274.
Pal, M., Mather, P.M., 2003. An assessment of the effectiveness of decision tree methods for land cover classification. Remote Sens. Environ. 86, 554–565. https://doi.org/10.1016/S0034-4257(03)00132-9.
Perennou, C., Guelmami, A., Paganini, M., Philipson, P., Poulin, B., Strauch, A., Tottrup, C., Truckenbrodt, J., Geijzendorffer, I.R., 2018. Chapter six - mapping Mediterranean wetlands with remote sensing: a good-looking map is not always a good map. In: Bohan, D.A., Dumbrell, A.J., Woodward, G., Jackson, M. (Eds.), Advances in Ecological Research. Academic Press, pp. 243–277. https://doi.org/10.1016/bs.aecr.2017.12.002.
Persson, M., Lindberg, E., Reese, H., 2018. Tree species classification with multi-temporal Sentinel-2 data. Remote Sens. 10, 1794. https://doi.org/10.3390/rs10111794.
Powell, R.L., Roberts, D.A., Dennison, P.E., Hess, L.L., 2007. Sub-pixel mapping of urban land cover using multiple endmember spectral mixture analysis: Manaus, Brazil. Remote Sens. Environ. 106, 253–267. https://doi.org/10.1016/j.rse.2006.09.005.
Ramsar Convention Secretariat, 2010. Water-related guidance: An integrated framework for the convention's water-related guidance. In: Ramsar Handbooks for the Wise Use of Wetlands, 4th edition. 8 Ramsar Convention Secretariat, Gland, Switzerland. https://www.ramsar.org/sites/default/files/documents/pdf/lib/hbk4-08.pdf.
Ramsar Convention Secretariat, 2018. Scaling up Wetland Conservation, Wise Use and Restoration to Achieve the Sustainable Development Goals. https://www.ramsar.org/sites/default/files/documents/library/wetlands_sdgs_e.pdf.
Rautiainen, M., Lukeš, P., Homolová, L., Hovi, A., Pisek, J., Mõttus, M., 2018. Spectral properties of coniferous forests: a review of in situ and laboratory measurements. Remote Sens. 10, 207. https://doi.org/10.3390/rs10020207.
Riiters, K.H., Wickham, J.D., Wade, T.G., 2010. Evaluating Anthropogenic Risk of Grassland and Forest Habitat Degradation Using Land-Cover Data. Landscape Online. 13. International Association for Landscape Ecology, Chapter Germany, Bonn, Germany, pp. 1–14. https://doi.org/10.3097/LO.200913.
Sanchez-Hernandez, C., Boyd, D.S., Foody, G.M., 2007. Mapping specific habitats from remotely sensed imagery: support vector machine and support vector data description based classification of coastal saltmarsh habitats. Ecological Informatics 2, 83–88. https://doi.org/10.1016/j.ecoinf.2007.04.003.
Singh, A., 1989. Review article digital change detection techniques using remotely-sensed data. Int. J. Remote Sens. 10, 989–1003. https://doi.org/10.1080/01431168908903939.
Singh, S.K., Srivastava, P.K., Szabó, S., Petropoulos, G.P., Gupta, M., Islam, T., 2017. Landscape transform and spatial metrics for mapping spatiotemporal land cover dynamics using earth observation data-sets. Geocarto International 32, 113–127. https://doi.org/10.1080/10106049.2015.1130084.
Smith, A., 2010. Image segmentation scale parameter optimization and land cover classification using the random Forest algorithm. J. Spat. Sci. 55, 69–79. https://doi.org/10.1080/14498596.2010.487851.
Tortora, R., 1978. A note on sample size estimation for multinomial populations. Am. Stat. https://doi.org/10.1080/00031305.1978.10479265.
Townshend, J.R.G., Justice, C.O., 1986. Analysis of the dynamics of African vegetation using the normalized difference vegetation index. Int. J. Remote Sens. 7, 1435–1445. https://doi.org/10.1080/01431168608948946.
UN Environment-Water, 2018. Progress on Water-Related Ecosystems, Piloting the Monitoring Methodology and Initial Findings for SDG Indicator 6.6.1. 978-92-807-3712-7.
USGS, 2017. Landsat Collections. https://landsat.usgs.gov/landsat-collections.
Vogt, P., Riitters, K., 2017. GuidosToolbox: universal digital image object analysis. European Journal of Remote Sensing 50, 352–361. https://doi.org/10.1080/22797254.2017.1330650.
Wang, L., Sousa, W.P., Gong, P., 2004. Integration of object-based and pixel-based classification for mapping mangroves with IKONOS imagery. Int. J. Remote Sens. 25, 5655–5668. https://doi.org/10.1080/014311602331291215.